

Overtone of H vibrations at Ni(111): Formation of delocalized states

H. Okuyama, T. Ueda, T. Aruga, and M. Nishijima*

Department of Chemistry, Graduate School of Science, Kyoto University, Kyoto 606-8502, Japan

(Received 12 October 2000; published 14 May 2001)

Vibrational states of H adsorbed on Ni(111) have been investigated by means of electron-energy-loss spectroscopy. In addition to the symmetric (v_s) and asymmetric (v_{as}) fundamental modes, the corresponding overtone structures are clearly detected. The overtone of v_{as} , the predominantly parallel-polarized mode, exhibits a doublet structure, which is interpreted to result from the delocalization of the excited vibrational states. It is shown that the doublet corresponds to the “bonding” and “antibonding” orbitals, analogous to the linear combination of atomic orbitals for simple molecules.

DOI: 10.1103/PhysRevB.63.233403

PACS number(s): 68.35.Ja, 73.20.Jc

I. INTRODUCTION

Atomic H adsorbed on metal surfaces is one of the most fundamental systems for examining the quantum nature of a particle. A proper description of a H atom on a surface is given by solving the Schrödinger equation with a two-dimensional periodic potential. Thus the vibrational eigenstates of H may be delocalized beyond the local potential well, giving rise to the “atomic band,” as predicted by Christmann *et al.*¹ Theoretical studies revealed that excited vibrational states of a H atom exhibit considerable delocalization on metal surfaces while the ground states are localized.^{2,3} Experimental studies have been carried out for, e.g., H/Rh(111),⁴ H/Cu(110),⁵ and H/Pd(110),⁶ by means of high-resolution electron-energy-loss spectroscopy (EELS). Typically, very low H coverages (below ~ 0.1 ML) were examined to realize a H atom in the extended periodic potential. However the EELS signals in such a low-coverage region were not always sufficient for the crucial observations of the delocalized states: the signal-to-noise ratio was small, and the effect of the surface contaminants (e.g., H_2O) was not completely eliminated.⁷

The picture of atomic bands is valid when the potential is periodic on the surface. If the H atom is allowed to be delocalized only within a finite region of the surface, the band picture is no longer valid. Instead, we should consider the vibrational states analogous to the electronic states of simple molecules. In this paper, we present a study on the vibrational states of H in two phases, i.e., (2×2) -2H and (1×1) -H, on Ni(111). In the former, a doublet was observed for the overtone of the predominantly parallel-polarized mode. We discuss the origin of the doublet, and attribute it to the formation of delocalized vibrational states.

II. EXPERIMENT

The experiments were carried out in an ultrahigh-vacuum chamber equipped with a high-resolution electron-energy-loss spectrometer (LK-5000, LK Technologies, Inc.), a four-grid retarding-field analyzer for low-electron energy diffraction (LEED), and a quadrupole mass spectrometer for gas analysis. A Ni(111) sample was cleaned in the manner described elsewhere.⁸ For a clean surface, a sharp 1×1 LEED

pattern was obtained, and the EELS showed no trace of impurity on the surface. The measurements were conducted at 90 K for the (2×2) -2H and (1×1) -H phases, with coverages of 0.5 and 1.0 ML, respectively.¹ The primary electron energies $E_p = 9.5$ and 17.5 eV, an incidence angle $\theta_i = 60^\circ$, an emission angle $\theta_e = 50^\circ$, and a typical energy resolution of 2 meV were used.

III. RESULTS

Figure 1(a) [1(b)] shows the EELS spectra for (2×2) -2H (D) on Ni(111). The peaks at 732 (554) and 1094

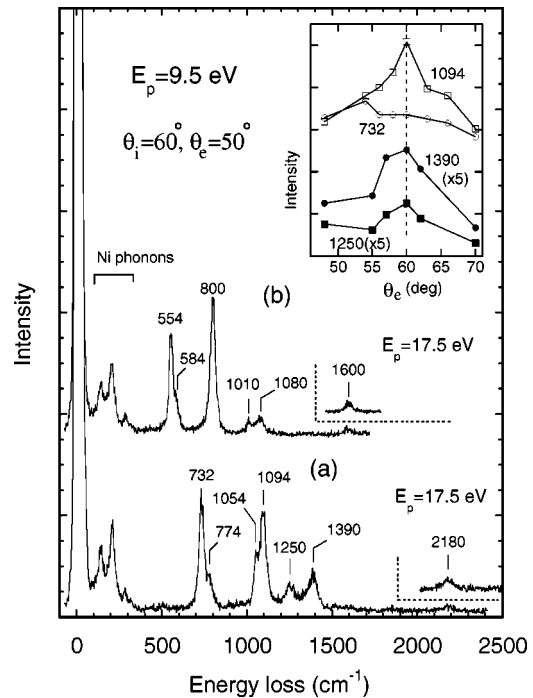


FIG. 1. EELS spectra for (a) (2×2) -2H and (b) (2×2) -2D phases on Ni(111). The primary electron energy $E_p = 9.5$ eV, incidence angle $\theta_i = 60^\circ$, and emission angle $\theta_e = 50^\circ$ were used. The high-energy-loss regions are also shown for $E_p = 17.5$ eV. The inset shows the emission-angle dependences of several loss intensities for (2×2) -2H, where each curve is vertically displaced for clarity.

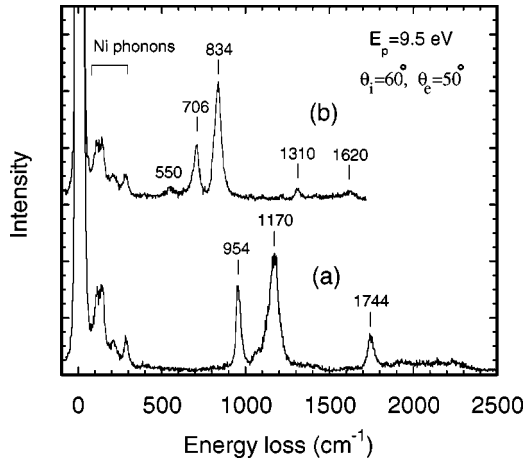


FIG. 2. EELS spectra for (a) (1×1) -H and (b) (1×1) -D phases on Ni(111). $E_p = 9.5$ eV, $\theta_i = 60^\circ$, and $\theta_e = 50^\circ$.

(800) cm^{-1} were previously observed, and assigned to the asymmetric (v_{as}) and symmetric (v_s) stretching vibrational modes of H (D) adsorbed in the three fold hollow sites, respectively.^{8–11} Due to the advanced sensitivity of the EELS spectrometer,¹² we can resolve the fundamental mode further. Peaks appear for H species at 774 and 1054 cm^{-1} in the higher- and lower-energy sides of the dominant losses (732 and 1094 cm^{-1}), respectively. The assignments are straightforward: there exist two kinds of adsorption sites for H in the (2×2) -2H phase, i.e., face-centered-cubic (fcc) and hexagonal-close-packed (hcp) hollow sites. The latter has a Ni atom below the adsorption site in the second layer, whereas the former does not. Although we cannot determine which loss pair is associated with the fcc or hcp sites, we tentatively denote the dominant losses at 732 and 1094 cm^{-1} as v_{as} and v_s , respectively, while the less intense losses at 774 and 1054 cm^{-1} as v'_{as} and v'_s , respectively. For D species, the corresponding asymmetric modes appear at 554 and 584 cm^{-1} , whereas the symmetric modes were hardly resolved and only a single loss was observed at 800 cm^{-1} .

In addition to these fundamental losses, we observed peaks at 1250 (1010), 1390 (1080) and 2180 (1600) cm^{-1} for H (D) species. The substantial isotope shifts rule out a contribution from the contamination (mainly H_2O) to these losses. The 2180 (1600) cm^{-1} peak is readily attributed to the overtone of v_s ($v_s^{(2)}$), judging from the energy. The origin of the two losses at 1250 (1010) and 1390 (1080) cm^{-1} will be discussed later.

The emission angle dependences of the loss intensities were examined to determine the vibrational mode symmetry.¹³ The results for H are shown in the inset of Fig. 1. The 1094- cm^{-1} loss has a broad peak in the specular direction, indicating a substantial contribution of the dipole scattering mechanism. This result reconfirms the previous assignments of the 1094 cm^{-1} loss as the symmetric mode of A_1 symmetry. The unidentified losses at 1250 and 1390 cm^{-1} similarly exhibit maxima in the specular direction and, thus, belong to the modes of A_1 symmetry.

Figure 2(a) [2(b)] shows the EELS spectra for (1×1) -H (D) on Ni(111). The asymmetric and symmetric modes are

shifted in energy and appear at 954 (706) and 1170 (834) cm^{-1} , respectively.^{8,10} In addition to these dominant losses, we observe a smaller peak at 1744 (1310) cm^{-1} , which is readily identified as $v_{as}^{(2)}$. This is in contrast to the case of the (2×2) -2H phase, where complex features are found. The broad structure ranging from 1900 to 2250 cm^{-1} in the H spectrum is interpreted as the two-phonon continuum of H overlayer.¹⁴ For D species, the small 550- cm^{-1} peak remains due to the imperfection of the 1×1 phase. The $v_s^{(2)}$ loss is resolved at 1620 cm^{-1} .

IV. DISCUSSION

Assignment of the two losses at 1250 (1010) and 1390 (1080) cm^{-1} as $v_{as}^{(2)}$ and $v'_{as}^{(2)}$ is unacceptable due to the relative weakness of the v'_{as} intensity. If one is assigned to $v_{as}^{(2)}$, the other should be ascribed to another fundamental mode. This is, however, inconsistent with the C_{3v} H-Ni configuration.¹¹ Under this configuration, we expect only two modes, i.e., one A_1 mode (symmetric) and one doubly degenerate E mode (asymmetric), to appear in EELS, which are already observed at 1094 and 732 cm^{-1} , respectively.

In some cases, however, the overtone of a fundamental loss may become a doublet. The 732 cm^{-1} loss is assigned as the doubly degenerate v_{as} of E symmetry and, thus, its overtone exhibits the representation $A_1 + E$. Hence the overtone may be split into a nondegenerate A_1 mode and a doubly degenerate E mode for oscillators with the potential for threefold symmetry. However, the angle-dependent measurements show that both losses belong to the A_1 symmetry, which is inconsistent with this interpretation. Also, the results for the (1×1) -H phase rule out this possibility: the degeneracy should be lifted even for the (1×1) -H phase if the threefold symmetry of the potential well is responsible for the splitting of the overtone. In addition, Fermi resonance coupling with v_s (A_1) may cause the splitting of the overtone ($A_1 + E$).¹⁵ This possibility is again ruled out by the angle-dependent measurements, as discussed above.

Another idea explaining the doublet feature is the delocalization of the vibrational states. To illustrate this idea qualitatively, we depict in Fig. 3(a) [3(b)] the adsorption structure of (2×2) -2H [(1×1) -H], and in Fig. 3(c), a one-dimensional cross section of the potential-energy surface of H in the (2×2) -2H phase along the lowest-energy path of the surface diffusion in the direction represented by the arrow in Fig. 3(a). In the (2×2) -2H phase [Fig. 3(a)], there are three vacant sites (denoted as site b) around the adsorption site (site a). Thus we represent the potential-energy diagram along the arrow by a double-minimum curve. This assumption will be discussed later. The activation energy of surface diffusion was investigated on Ni(111) and determined to be ~ 200 meV (1600 cm^{-1}) at ~ 0.3 ML.¹⁶ The diffusion along the surface-parallel direction is related to the parallel-polarized vibrations, i.e., $v_{as}^{(n)}$. The second-excited state ($v_{as}^{(2)}$) lies in the range of 1150–1500 cm^{-1} , and is comparable with the potential barrier, giving rise, possibly, to delocalized vibrational states. The delocalization of vibrational states within the multiple potential wells would result

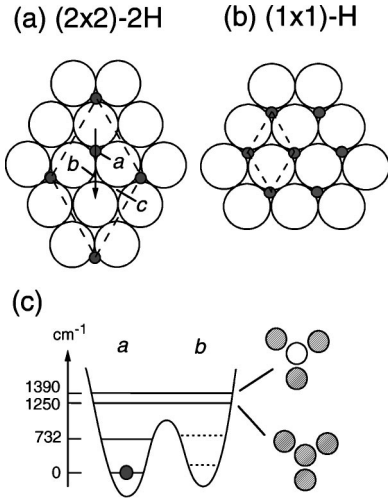


FIG. 3. Schematic adsorption geometries for (a) (2×2) -2H and (b) (1×1) -H phases on Ni(111). The large open circles represent Ni atoms, and the small shaded circles H atoms. The dashed hexagons show the surface unit meshes. The potential-energy diagram for the (2×2) -2H phase is represented in (c) by the one-dimensional cross section along the arrow depicted in (a). Two delocalized vibrational eigenfunctions are represented by the combinations of the spherical functions.

in the formation of the “bonding” and “antibonding” states. Hence we propose that the doublet observed for $v_{as}^{(2)}$ is ascribed to the transition of H from the localized ground state to the delocalized excited states. The vibrational properties of H in the (1×1) -H phase strongly support this proposal, where only a single peak is observed for $v_{as}^{(2)}$. The corresponding adsorption structure is shown in Fig. 3(b). In this case, the nearest-neighbor site exhibits a steep barrier due to the repulsive H-H interactions,¹⁷ which promotes the localization of the excited state.

To understand the vibrational delocalization in more detail, we demonstrate a simple calculation. The Hamiltonian H , associated with the $v_{as}^{(2)}$ state, is given by

$$H = \sum_{i=1}^4 \varepsilon_i c_i^\dagger c_i + \sum_{i,j=1}^4 \Delta_{ij} c_i^\dagger c_j, \quad (1)$$

where ε_i is the zeroth-order vibrational energy associated with the i th site, c_i^\dagger (c_i) is the creation (annihilation) operator for the site i , and Δ_{ij} is the hopping matrix element between sites i and j . The index $i=1$ corresponds to the site a and the others ($i=2-4$) to sites b [Fig. 3(a)]. The energy eigenvalues of this Hamiltonian are obtained by diagonalizing the 4×4 matrix, the matrix elements of which are

$$H_{11} = \varepsilon_a, \quad H_{ii} = \varepsilon_b, \quad H_{1i} = H_{i1} = \Delta, \quad (2)$$

with $i=2, 3$, and 4 , and the other matrix elements equal to zero. We consider the interactions (Δ_{ij}) only between the nearest-neighbor sites. Analogously to the procedure of the linear combination of atomic orbitals for simple molecules, this is easily solved to give the eigenvalues of $(\varepsilon_a + \varepsilon_b)/2 \pm \sqrt{[(\varepsilon_a - \varepsilon_b)/2]^2 + 3\Delta^2}$ and ε_b , which correspond to the antibonding (A_1), bonding (A_1), and doubly degenerate

nonbonding (E) states, respectively. Due to its nonbonding character, the wave function of the E -symmetry states is localized at the sites b , and thus has little spatial overlap with the ground-state wave function (localized at site a). This indicates that the excitations from the ground state to these nonbonding states are suppressed.¹⁸ Hence the losses observed at 1250 and 1390 cm^{-1} are likely attributed to the transitions to the bonding (A_1) and antibonding (A_1) states, respectively [see Fig. 3(c)], which is consistent with the emission-angle dependencies of the loss intensities. We can deduce $|\Delta|$ from the observed splitting energies to be ~ 40 and 20 cm^{-1} for H and D, respectively, if we assume $\varepsilon_a \approx \varepsilon_b$. These values are comparable with those determined to be 73 and 20 cm^{-1} for H and D, respectively, on Cu(110),⁵ and 40 cm^{-1} for H on Pd(110).⁶

We will make a qualitative discussion on the potential energy surface drawn in Fig. 3(c). Sites a and b are not equivalent because of the existence of the fcc and hcp sites on the surface. However, the difference in the adsorption (or zero-point) energies of a H atom between the fcc and hcp sites are predicted to be only ~ 10 meV.¹⁹ The adsorption energies of H at sites a and b are affected by the H-H interactions. The difference in the adsorption energies of a H atom between (1×1) -H and (2×2) -2H is ~ 50 meV,^{1,19} and thus the energy difference due to the H-H interactions is considered to be at most ~ 50 meV. Because these values are small as compared to the barrier energy of ~ 200 meV, it is plausible to describe the potential energy of H for the (2×2) -2H phase with a double-minimum curve, as depicted in Fig. 3(c). Note that the population of the next-nearest-neighbor sites (site c) is significantly more unfavorable due to the strong repulsions by the neighboring H adatoms.

The perpendicular-polarized $v_s^{(2)}$ in the (2×2) -2H phase exhibits only a single-loss peak and, thus, the excited state is considered to be localized. It is notable that the vibrational delocalization is mode specific, and observed exclusively for the parallel-polarized mode, whose vibrational wave function is extended laterally on the surface. This indicates that a considerable overlap of the wave functions is essential for a delocalization of the vibrational states.

The delocalized nature of the vibrational states is closely associated with the energy-level positions with respect to the barrier top. Indeed, typical vibrational energies of H on the transition-metal surfaces are in the range from ~ 450 to 1300 cm^{-1} ,¹ and are comparable with the typical activation energy of surface diffusion,^{16,20} as noted above. Hence the vibrational delocalization is a general nature of H on transition metal surfaces.

Finally, our results show that delocalization can be observed even at a high coverage (0.5 ML), where it was believed that the repulsive interactions between H adatoms promote the localization.^{5,6} Considering the difficulties of the low-coverage (below 0.1 ML) experiments due to, e.g., very low signal intensities, more convincing experiments in the submonolayer range will facilitate the understanding of the delocalized nature of H vibrational states.

V. SUMMARY

In summary, we observed a doublet structure for the overtone of the asymmetric stretching mode (the predominantly parallel-polarized mode). Considering that the vibrational energies are comparable with the activation energy of surface diffusion, we attribute the doublet to the delocalization of the vibrationally excited states. The coverage dependences and angle-dependent measurements, as well as the prominent

mode specificity, strongly verify the quantum-delocalized picture of the vibrational states.

ACKNOWLEDGMENTS

This work was supported in part by a Grant-in-Aid from the Ministry of Education, Science, Sports and Culture (Japan).

*Corresponding author telephone: +81-75-753-3979, fax: +81-75-753-4000, e-mail: nishijima@kuchem.kyoto-u.ac.jp

¹K. Christmann, R. J. Behm, G. Ertl, M. A. Van Hove, and W. H. Weinberg, *J. Chem. Phys.* **70**, 4168 (1979).

²M. J. Puska, R. M. Nieminen, M. Manninen, B. Chakraborty, S. Holloway, and J. K. Nørskov, *Phys. Rev. Lett.* **51**, 1081 (1983); M. J. Puska and R. M. Nieminen, *Surf. Sci.* **157**, 413 (1985).

³S. W. Rick and J. D. Doll, *Surf. Sci.* **302**, L305 (1994).

⁴C. M. Mate and G. A. Somorjai, *Phys. Rev. B* **34**, 7414 (1986).

⁵C. Astaldi, A. Bianco, S. Modesti, and E. Tosatti, *Phys. Rev. Lett.* **68**, 90 (1992).

⁶N. Takagi, Y. Yasui, T. Takaoka, M. Sawada, H. Yanagita, T. Aruga, and M. Nishijima, *Phys. Rev. B* **53**, 13 767 (1996).

⁷H. Yanagita, H. Fujioka, T. Aruga, N. Takagi, and M. Nishijima, *Surf. Sci.* **441**, 507 (1990).

⁸H. Yanagita, J. Sakai, T. Aruga, N. Takagi, and M. Nishijima, *Phys. Rev. B* **56**, 14 952 (1997).

⁹W. Ho, N. J. DiNardo, and E. W. Plummer, *J. Vac. Sci. Technol.* **17**, 134 (1980).

¹⁰K. J. Maynard, A. D. Johnson, S. P. Daley, and S. T. Ceyer,

Faraday Discuss. Chem. Soc. **91**, 437 (1991).

¹¹G. Gross and K. H. Rieder, *Surf. Sci.* **241**, 33 (1991).

¹²H. Ibach, *J. Electron Spectrosc. Relat. Phenom.* **64/65**, 819 (1993).

¹³H. Ibach and D. L. Mills, *Electron Energy Loss Spectroscopy and Surface Vibrations* (Academic, New York, 1982).

¹⁴H. Okuyama, T. Ueda, T. Aruga, and M. Nishijima, following paper, *Phys. Rev. B* **63**, 233404 (2001).

¹⁵G. Herzberg, *Molecular Spectra and Molecular Structure II, Infrared and Raman Spectra of Polyatomic Molecules* (Van Nostrand, Princeton, 1945).

¹⁶G. X. Cao, E. Nabighian, and X. D. Zhu, *Phys. Rev. Lett.* **79**, 3696 (1997).

¹⁷P. Nordlander and S. Holmström, *Surf. Sci.* **159**, 443 (1985).

¹⁸N. V. Richardson and N. Sheppard, in *Vibrational Spectroscopy of Molecules on Surfaces*, edited by J. T. Yates, Jr. and T. E. Maday (Plenum, New York, 1987).

¹⁹G. Kresse and J. Hafner, *Surf. Sci.* **459**, 287 (2000).

²⁰R. Gomer, *Rep. Prog. Phys.* **53**, 917 (1990).